Phosphorylation-Induced Conformational Changes in Short Peptides Probed by Fluorescence Resonance Energy Transfer in the 10 Angstrom Domain

ARTICLE *in* CHEMBIOCHEM · MARCH 2007

Impact Factor: 3.09

2 AUTHORS:

Harekrushna Sahoo
National Institute of Technology Rourkela
14 PUBLICATIONS **84** CITATIONS
SEE PROFILE

Werner M Nau
Jacobs University
307 PUBLICATIONS **7,376** CITATIONS
SEE PROFILE

DOI: 10.1002/cbic.200600466

Phosphorylation-Induced Conformational Changes in Short Peptides Probed by Fluorescence Resonance Energy Transfer in the 10 Å Domain

Harekrushna Sahoo and Werner M. Nau*[a]

*Phosphorylation-induced conformational changes in short polypeptides were probed by a fluorescence resonance energy transfer (FRET) method by employing a short-distance FRET pair ($R_0 \approx 10$ Å) based on tryptophan as natural donor and a 2,3-diazabicyclo[2.2.2]oct-2-ene-labeled asparagine (Dbo) as synthetic acceptor. Two substrates for kinases, LeuArgArgTrpSerLeuGly-Dbo (peptide **I**) and TrpLysArgThrLeuArgArg-Dbo (peptide **II**), were investigated, with serine and threonine, respectively, as phosphorylation sites. Steady-state and time-resolved fluorescence experiments in H_2O revealed a decrease in FRET efficiency for peptide **I** and an increase for peptide **II**; this suggested that the effective distances between donor and acceptor increased and decreased, respectively. The same trends and similar absolute variations in effective donor–acceptor distances were observed in propylene glycol, a less polar and highly viscous solvent; this suggested that the variations are due to intrinsic structural preferences. Fitting of the time-resolved decay traces according to a distribution function model (Gaussian distribution) provided the mean donor–acceptor distances, which showed an increase upon phosphorylation for peptide **I** (from 9.7 to 10.5 Å) and a decrease for peptide **II** (from 10.9 to 9.3 Å) in H_2O. The broadness (half-width) of the distributions, which provides a measure of the rigidity of the peptides, remained similar upon phosphorylation of peptide **I** (3.0 versus 3.1 Å), but decreased for peptide **II** (from 3.1 to 0.73 Å in H_2O); this suggests a more compact, structured conformation upon phosphorylation of the latter peptide. The elongation of the peptide backbone (by ca. 0.7 Å) for peptide **I** is attributed to an increase in steric demand upon phosphorylation, which favors an extended conformation. The contraction (by ca. 1.4 Å) and structural rigidification of peptide **II** is attributed to attractive Coulombic interactions and hydrogen bonding between the phosphate group and the arginine residues.*

Introduction

Protein phosphorylation is an important biological process at the intracellular level that is responsible for several vital functions through the regulation of metabolic pathways, including gene transcription and translation,[1] cell growth,[2] and others.[3,4] Phosphorylation occurs at the hydroxyl group of serine, threonine, and tyrosine in eukaryotic cells, thereby converting it to a sterically more demanding, doubly charged phosphate group ($pK_a \approx 6.7$).[5] This chemical modification leads to concomitant changes in the structural and conformational properties of proteins, for example, through Coulombic interactions, changes in hydrogen bonding, or steric effects,[6,7] which are directly or indirectly held responsible for the biological activity of phosphorylated peptides or proteins.[8–11]

The phosphorylation of serine and threonine, which are investigated herein, is presumed to contribute more than 99% to the total phosphorylation events,[7] and frequently multiple phosphorylation of several serine and threonine residues in a protein occurs.[12] The conformational changes accompanying serine or threonine phosphorylation, which are of prime interest for their biological effects, have previously been investigated by X-ray crystallography[13] and electron microscopy[14] in the solid state, and by NMR,[15] fluorescence,[6] and CD spectroscopy[7] in solution. The experimental studies have been complemented by molecular-dynamics simulations.[6,16,17]

We have studied by fluorescence resonance energy transfer (FRET) the changes in donor–acceptor distances upon the phosphorylation of serine and threonine in two short model peptides[18] by making use of a recently communicated donor–acceptor pair with superior performance at short distances.[19] This allowed us to study the conformational changes with high precision for peptides that represent only the fundamental recognition sequences for kinases and that are sufficiently short to be considered as random coiled. We observed an interesting contrast between the two peptides, with an elongation of the peptide length in one case and a contraction in effective distance in the other one. The novel FRET pair[19] employs tryptophan as intrinsic donor and the synthetic amino acid Dbo (2,3-diazabicyclo[2.2.2]oct-2-ene-labeled asparagine) as acceptor.

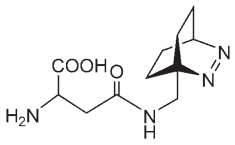

Dbo

[a] *Dr. H. Sahoo, Prof. W. M. Nau*
School of Engineering and Science, Jacobs University Bremen
Campus Ring 1, 28759 Bremen (Germany)
Fax: (+49) 421-200-3229
E-mail: w.nau@iu-bremen.de

Results and Discussion

As demonstrated in our preliminary study,[19] the Trp/Dbo FRET pair has an exceptionally small critical transfer distance of about 10 Å, which allows the determination of distances in short (< 20 amino acids) peptides with high accuracy. It should therefore be possible to investigate effective donor–acceptor distances and distance distributions in isolated recognition motifs, and also to assess the effects of subtle structural changes on the donor–acceptor distances. This would provide a convenient spectroscopic tool for determining whether intrinsic factors (structural modifications, mutations) or extrinsic factors (salt effects, pH, temperature) lead to an elongation or contraction of the (average) peptide conformation, namely the effective distance between donor and acceptor. Note also that the acceptor (Dbo) does not absorb at the excitation wavelength of the donor (Trp, $\lambda_{ex} = 280$ nm);[19] this simplifies the experimental design. For example, it allows for direct adjustment and accurate matching of the donor absorbance for steady-state state experiments without correction for residual acceptor absorbance.

This study deals with the effects of a chemical modification, namely phosphorylation in the peptide backbone, because the accompanying changes of peptide conformation and dynamics are frequently implicated in their biological effects.[8–11] We designed the model peptides according to the recognition motifs of two important kinases, protein kinase A (peptide **I**) and protein kinase C (peptide **II**).[20,21] The sequences of the unphosphorylated peptides (**I** and **II**), their phosphorylated counterparts (**pI** and **pII**), and the corresponding reference peptides (**ref-I** and **ref-II**, for determination of FRET efficiencies) employed in this study are shown in Table 1. The peptides were

Table 1. Sequences of peptides employed in this study.

peptide **I**:	LeuArgArgTrp-Ser-LeuGlyDbo
peptide **pI**:	LeuArgArgTrp-pSer-LeuGlyDbo
peptide **II**:	TrpLysArg-Thr-LeuArgArgDbo
peptide **pII**:	TrpLysArg-pThr-LeuArgArgDbo
peptide **ref-I**:	LeuArgArgTrp-Ser-LeuGly-NH_2
peptide **ref-II**:	Trp-$(Lys)_6$-NH_2

obtained by solid-phase synthesis, by employing Fmoc-protected Dbo; this allowed for sufficient amounts (5 mg) and purity (> 95 %). Owing, among other things, to the small size and high hydrophilicity of Dbo,[22–25] all peptides showed sufficient solubility (> 100 μM) in both water and propylene glycol.

Dbo, as FRET acceptor, was introduced at the C termini of the model peptides, while Trp, as donor, was either at an internal position (**I**) or at the N terminus (**II**). Accordingly, donor and acceptor were separated by 3–6 amino acids, one of which was the one predisposed for phosphorylation (Ser or Thr, underlined in Table 1). Note that the phosphorylation of serine (**I**) or threonine (**II**) corresponds only to a small chemical modification, as illustrated in Scheme 1. However, it can result in sizable structural variations.

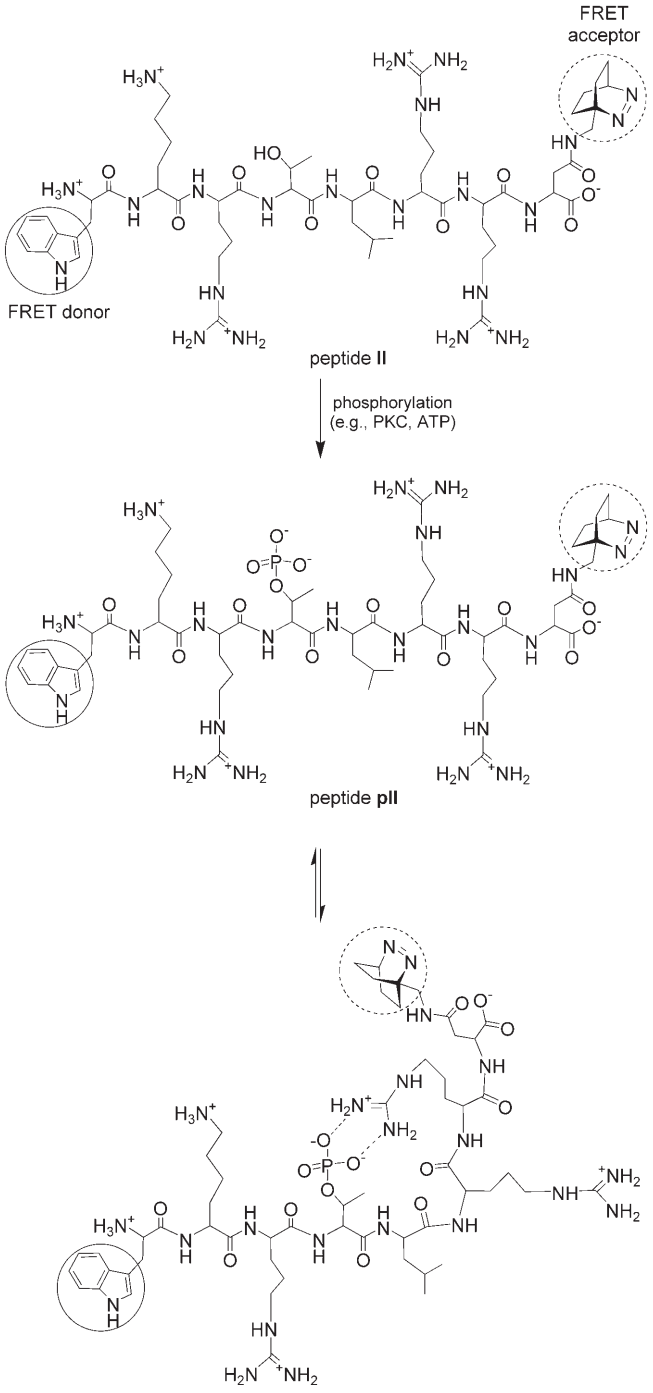

Scheme 1. Chemical modifications and presumed structural changes that accompany the phosphorylation of peptide **II**.

Intramolecular FRET efficiencies and donor–acceptor distances were measured for peptides **I**, **pI**, **II**, and **pII**. For **I** and **pI**, the isostructural **ref-I** (without Dbo) was designed as reference, because the fluorescence of the internal Trp was expected to depend strongly on both neighboring amino acids. For peptides **II** and **pII**, we used an available reference sample, **ref-II**, because the fluorescence of N-terminal Trp residues depends mainly on the immediate neighbor (Lys in this case).[26] Note, the qualitative conclusions and trends established herein are

independent of the choice of the reference peptide, because we focus on the relative changes upon phosphorylation.

The spectral overlap values (determined from the Trp emission and Dbo absorption spectra),[19] fluorescence quantum yields (determined with reference to that of Trp, $\Phi_f = 0.13$ in H_2O),[27] and the resulting critical transfer radii (R_0, Förster distances) are collected in Table 2. R_0 is defined as the distance at which half of the energy is transferred from donor to acceptor. The characteristic R_0 value of the Trp/Dbo FRET pair (ca. 10 Å)[19] is slightly modulated by the different fluorescence quantum yields of Trp in different peptides (cf. **ref-I** with **ref-II**) and solvents (Table 2). In particular, a neighboring arginine is known to be a moderate intramolecular fluorescence quencher of Trp;[28] this might account for the lower fluorescence quantum yield of peptide **ref-I** in both solvents.

The fluorescence intensities and lifetimes (Figure 1) for the donor–acceptor-labeled peptides were smaller than those for the donor-only labeled peptides; this suggests sizable FRET. The FRET efficiencies (E, Table 3) were determined from the decrease in fluorescence intensity ($E = 1 - I_{DA}/I_D$) and lifetime[19] ($E = 1 - \tau_{DA}/\tau_D$) of the peptide in the presence (I_{DA}, τ_{DA}) and absence (I_D, τ_D) of the acceptor. Note that the fluorescence decays of Trp in all peptides were not monoexponential; a biexponential decay function was satisfactory for fitting ($\chi^2 < 1.1$), and the resulting dual lifetimes (τ) and their contributions (pre-exponential factor α) are contained in Table 4 as raw data. In the calculations of the time-resolved FRET efficiencies (Table 3) we employed the average lifetimes (τ_{av}) for consistency.[19] Most importantly, the FRET effi-

Table 2. Photophysical parameters of the Trp/Dbo FRET pair obtained for the donor-only- and acceptor-only-substituted reference peptides in different solvents

Donor	Acceptor	Solvent	J [10^{11} M^{-1} cm^{-1} nm^4][a]	ϕ_D[b]	R_0 [Å][c]
ref-I[d]	$(GlySer)_6$-Dbo	H_2O	5.09	0.07	9.35
		propylene glycol	4.01	0.13	9.49
ref-II[e]	$(GlySer)_6$-Dbo	H_2O	5.09	0.12	10.13
		propylene glycol	4.01	0.21	10.31

[a] Spectral overlap between fluorescence of donor and absorption of acceptor. [b] Fluorescence quantum yield of donor determined with reference to Trp ($\Phi_f = 0.13$ in H_2O.[27]) [c] Critical transfer radius, see ref. [19] for further details of the calculation. [d] LeuArgArgTrpSerLeuGly-NH_2, reference for peptides **I** and **pI**. [e] Trp-$(Lys)_6$-NH_2, reference for peptides **II** and **pII**.

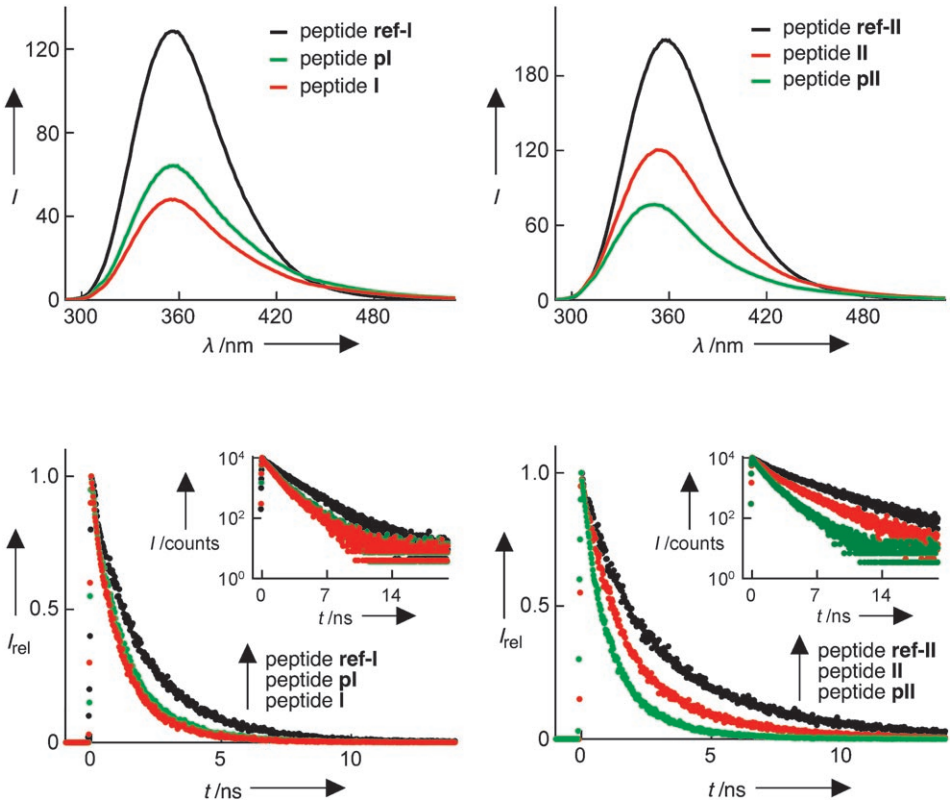

Figure 1. Steady-state fluorescence spectra (top) and fluorescence decay traces (bottom, inset: logarithmic intensity scale) for peptide **I** (left) and peptide **II** (right) in their unphosphorylated (red) and phosphorylated (green) forms in H_2O. The fluorescence spectra of the reference peptides (without acceptor) are shown in black.

Table 3. Effective transfer distances obtained from steady-state and time-resolved FRET measurements

Peptide	Method	H_2O			Propylene glycol		
		E[a]	F[b]	R_{eff} [Å][c]	E[a]	F[b]	R_{eff} [Å][c]
I	steady-state	0.62	0.20	8.6	0.46	0.13	9.7
	time-resolved	0.42		8.7	0.33		9.8
pI	steady-state	0.50	0.14	9.4	0.36	0.10	10.4
	time-resolved	0.36		9.4	0.26		10.5
II	steady-state	0.42	0.02	10.7	0.33	0.11	11.6
	time-resolved	0.40		10.7	0.22		11.8
pII	steady-state	0.63	0.02	9.3	0.50	0.20	10.3
	time-resolved	0.61		9.3	0.30		10.3

[a] FRET efficiency; 5% error. [b] Static-quenching component. [c] Effective donor–acceptor distance calculated according to Equation (1) (steady-state) or Equation (2) (time-resolved); error ±0.3 Å.

Table 4. Fluorescence lifetimes of the reference and labeled peptides.

peptide	H_2O			propylene glycol		
	τ [ns][a]	α[b]	τ_{av} [ns][c]	τ [ns][a]	α[b]	τ_{av} [ns][c]
I	0.86	0.77	1.05	1.69	0.58	2.80
	1.71	0.23		4.32	0.42	
pI	0.86	0.69	1.15	1.79	0.56	3.06
	1.79	0.31		4.66	0.44	
ref-I	1.00	0.36	1.80	2.59	0.46	4.19
	2.26	0.64		5.56	0.54	
II	1.05	0.72	1.63	1.93	0.50	2.88
	3.10	0.28		3.82	0.50	
pII	0.79	0.72	1.07	1.72	0.49	2.58
	1.79	0.28		3.40	0.51	
ref-II	1.43	0.56	2.73	2.47	0.52	3.69
	4.35	0.44		4.99	0.48	

[a] Fluorescence lifetimes obtained from biexponential fitting. [b] Pre-exponential factors of the two lifetime components ($\alpha_1+\alpha_2\equiv 1$). [c] Average fluorescence lifetime calculated as $\tau_{av}=\alpha_1\tau_1+\alpha_2\tau_2$.

ciencies in Table 3 lie in the ideal range of 20–80%, that is, FRET is highly significant, considering typical errors, but far from quantitative. This allows for particularly accurate measurements and establishes Trp/Dbo as the donor/acceptor pair of choice for distance measurements in these short peptides.

The steady-state FRET efficiency (E_{ss}) for **I** in H_2O (0.62, Figure 1) decreased upon going to the phosphorylated form **pI** (0.50). The same trend was found in propylene glycol (0.46 and 0.36 for the unphosphorylated and phosphorylated peptides, respectively). The lower absolute FRET efficiencies in propylene glycol can be attributed to a solvent effect on the peptide conformation and/or the absence of diffusion-enhanced FRET in this highly viscous solvent (45 times higher viscosity than H_2O).[19] Interestingly, for **II**, the steady-state FRET efficiency increased upon phosphorylation in both H_2O (from 0.42 to 0.63, Figure 1) as well as in propylene glycol (from 0.33 to 0.50). Peptides **I** and **II** therefore display contrasting conformational changes in response to phosphorylation, and this can be qualitatively interpreted in terms of an elongation for **I** (decreased FRET) and a contraction for **II** (increased FRET) [Eq. (1)]:

$$R_{eff} = \sqrt[6]{R_0^6\left(\frac{1}{E_{ss}}-1\right)} \qquad (1)$$

The E_{ss} values were used to calculate the effective donor–acceptor distances (R_{eff}, neglecting distance distributions and static quenching, see below) according to Equation (1), which are given in Table 3. The variations in steady-state FRET efficiencies in H_2O reveal that the R_{eff} value increased by about 0.8 Å for **I** and decreased by about 1.4 Å for **II**. These changes are significant, also in propylene glycol, especially if one considers the short absolute donor–acceptor separations in these small peptides (ca. 10 Å).

The time-resolved FRET efficiencies (E_{tr}) were consistently smaller than the steady-state FRET efficiencies (Table 3). This is characteristic for short peptides, in which a significant fraction of the conformational subpopulations can be in intimate donor–acceptor contact[29,30] when excitation occurs.[19] Because this fraction undergoes static quenching, it contributes to the observed FRET efficiency in the steady-state, but not in the time-resolved experiments, owing to the limited time resolution. Consequently the fraction of static quenching ($F=E_{ss}-E_{tr}$) can be defined as the difference between the two FRET efficiencies. As can be seen (Table 3), static quenching accounts for 2–20% of the steady-state FRET efficiency, but the variations are too small and too irregular to allow further conclusions to be drawn about the solvent dependence of the static-quenching fraction or its variation in dependence on phosphorylation.

Apart from the variations due to static quenching, the time-resolved FRET efficiencies in both solvents revealed similar trends to those observed for the steady-state experiments. The average fluorescence lifetimes increased slightly (by ca. 10% in H_2O, Table 4 and Figure 1) but significantly upon phosphorylation of peptide **I**, corresponding to a lower FRET efficiency and an increased donor–acceptor separation (Table 3). In contrast, for peptide **II**, the average fluorescence lifetime decreased (by 35% in H_2O, Table 4 and Figure 1) resulting in a higher FRET efficiency and suggesting a shorter donor–acceptor separation (Table 3). In order to calculate the effective donor–acceptor distances from the average fluorescence lifetimes, and to directly compare them with the R_{eff} values obtained from the steady-state experiments, corrections for the static quenching component are required. Equation (2) weights the latter fraction by assuming a van der Waals contact distance (R_{vdW}) of 4.0 Å (from molecular dynamics calculations)[29,30] for the pairs already in contact when excitation occurs.[19]

$$R_{eff} = (1-F)\sqrt[6]{R_0^6\left(\frac{1}{E_{tr}}-1\right)} + FR_{vdW} \qquad (2)$$

As can be seen, the R_{eff} values obtained in this manner from the time-resolved data (Table 3) are in excellent agreement with the steady-state results; this again confirms that the donor–acceptor separation for **I** increases on average (by ca. 0.7 Å) and that of **II** decreases (by ca. 1.4 Å) in both solvents.

Peptides **I** and **II** are not expected to adapt a stable secondary structure, but to mainly exist in random-coiled conformations. Consequently, the donor–acceptor separation is better described by a distribution, $P(R)$, than by a single average value (like the R_{eff} values derived from the steady-state FRET efficiencies, see above). As exemplified in a preliminary report for flexible Gly-Ser repeat peptides,[19] time-resolved fluorescence decays can be employed to derive such distribution functions for peptides by assuming either a Gaussian or a worm-like chain distribution function. In this work, we fitted a Gaussian distribution to the decay traces according to Equation (3).[27,31–34]

$$I_{DA}(t) = I_D^0\int_0^\infty P(R)\sum_i \alpha_i \exp\left[-\frac{t}{\tau_{D,i}}\left(1+\left(\frac{R_0}{R}\right)^6\right)\right]dR \qquad (3)$$

$$\text{with } P(R) = \frac{1}{\sigma\sqrt{2\pi}}\exp\left[-\frac{1}{2}\left(\frac{R-R_{mean}}{\sigma}\right)^2\right]$$

$I_{DA}(t)$ is the time-dependent fluorescence intensity, I_D^0 is the fluorescence intensity at $t=0$, $\tau_{D,i}$ and α_i are the individual fluorescence lifetime components and their contributions in the absence of acceptor (of the reference peptides, see Table 4), R_{mean} is the maximum of the Gaussian function, and σ is the standard deviation, which is related to the half-width of the distribution (full width at half maximum, hw) as $hw = 2.354\sigma$.

The distribution functions recovered from fits of Equation (3) are depicted in Figure 2 for H_2O and propylene glycol. In analogy to our previous study,[19] we have also included the static quenching components (short-distance peaks in Figure 2) derived from the FRET efficiencies (F values) by again assuming a van der Waals contact distance of 4 Å (see above) and, arbitrarily, a half-width of 1 Å for this component. Diffusion-enhanced FRET is expected to interfere in the case of H_2O as solvent,[19] and can introduce a systematic error into the corresponding distributions (shift them to apparently too short distances, in particular). Nevertheless, the qualitative appearance of the distributions in the two solvents and their relative variations accompanying phosphorylation (dashed lines), or when comparing peptide **I** (left) with **II** (right), are similar. As was found for the R_{eff} values directly obtained from the FRET efficiencies (Table 3), the R_{mean} values recovered from analysis of the Gaussian distribution function (Table 5) increase upon phosphorylation of **I**, for example, from 9.7 to 10.5 Å in H_2O, but decrease for **II**, for example, from 10.9 to 9.3 Å in H_2O.

Comparison of the R_{mean} values recovered in propylene glycol (Table 5) with existing literature values[19] is instructive. For **I** and **pI** in propylene glycol and in which donor (Trp) and acceptor (Dbo) are separated by three amino acids (SerLeuGly), the R_{mean} values are 11.2 and 12.2 Å, respectively. For **II** and **pII**, in which donor and acceptor are separated by six amino acids (LysArgThrLeuArgArg), they are 12.3 and 11.5 Å. For comparison, the mean donor–acceptor separations (R_{mean}), previously determined by the same FRET technique for the random-coiled peptides Trp-(GlySer)$_n$-Dbo-NH_2 with two ($n=1$) to eight ($n=4$) intervening flexible amino acids, span 10.6–12.9 Å,[19] while for the extended peptide Trp-Pro_6-Dbo-NH_2, with six intervening rigid prolines, it amounts to 15.3 Å.[35] The determined distances for the presently investigated peptides therefore fall into the expected range for flexible or semiflexible peptides, but below the mean distance for an extended conformation. However, a more detailed comparison of the absolute distances is not possible due to the variations in the amino acid type (and in the case of peptide **I** also the presence of the dangling N-terminal end).

Table 5. Recovered distance distribution parameters (Gaussian function).[a]

peptide	hw [Å][b]		R_{mean} [Å][c]	
	H_2O	propylene glycol	H_2O	propylene glycol
I	3.0	1.6	9.7	11.2
pI	3.1	2.0	10.5	12.2
II	3.1	1.2	10.9	12.4
pII	0.73	0.23	9.3	11.5

[a] Obtained from fitting of the time-resolved fluorescence decays according to Equation (3). [b] Full width at half maximum height; 10% error. [c] Mean donor–acceptor separation and maximum of Gaussian distribution function; error ±0.3 Å.

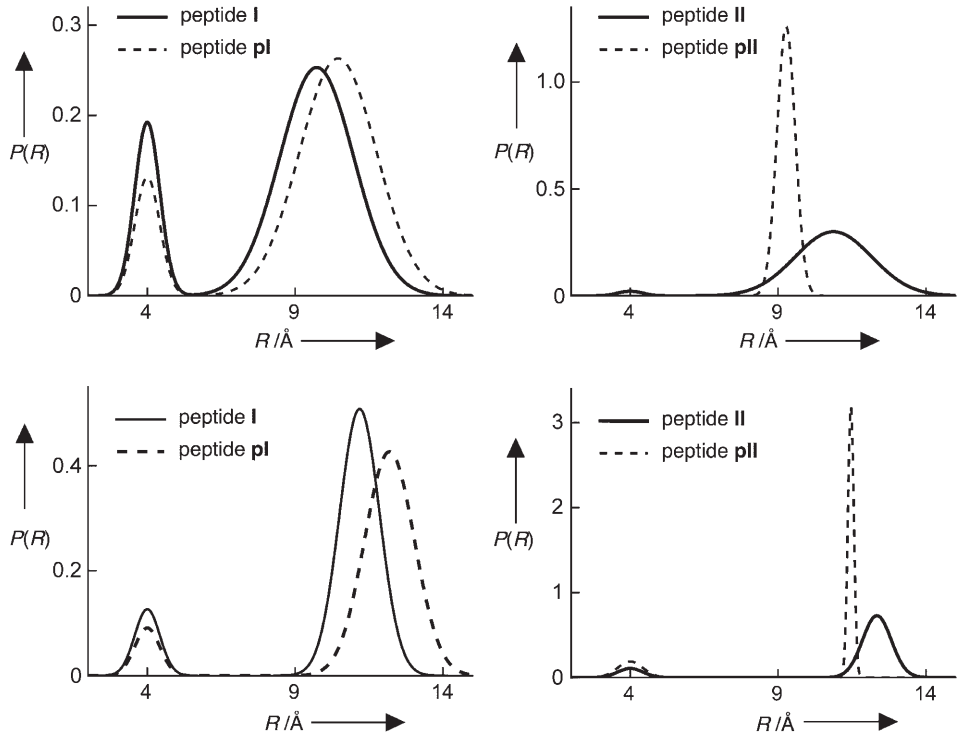

Figure 2. Gaussian distribution functions recovered for the donor–acceptor distance of peptides **I** and **pI** (left) and peptides **II** and **pII** (right) in H_2O (top) and propylene glycol (bottom).

The absolute values of the mean distances also revealed exceptional behavior. The *unphosphorylated* peptide **II** has a larger mean donor–acceptor separation than **I** (12.4 vs. 11.2 Å in propylene glycol), as expected from the larger number of amino acids (6 vs. 3) separating donor and acceptor.[19] The *phosphorylated* peptide **pII**, however, has a slightly shorter R_{mean} value than peptide **pI** (11.5 vs. 12.2 Å), which cannot be rationalized in terms of the established length dependence.[19] The simplest explanation for this observation is that peptide **pII** adapts a contracted conformation (see above).

An additional quintessential piece of information (besides the trends in mean distances, that is, maxima of the Gaussian function) can be obtained from the shape of the distributions upon phosphorylation, which remains

similar for peptide **I**, but becomes much sharper for peptide **II** (Figure 2). Quantitatively, the broadness of the distribution is described by the half-width, which provides a measure of the flexibility of the peptide. The recovered hw values (Table 5) range from 1–2 Å for peptides **I**, **pI**, and **II**. This falls below the range of 2.8–5.3 Å recovered for the similarly long but highly flexible Trp-(GlySer)$_n$-Dbo-NH$_2$ peptides ($n=2$–4),[19] but above the range of 0.1–1.0 for rigid polyprolines, TrpPro$_n$Dbo-NH$_2$ ($n=2$–6),[35] thus suggesting that these peptides are semiflexible. This is also consistent with the presumed random-coiled conformation.[36] An exception is the phosphorylated peptide **pII**, which shows a very narrow spike in the distribution and therefore a very small half-width (0.23 Å) that is indicative of a rigid, more highly structured peptide with a more uniform donor–acceptor separation. In other words, phosphorylation of this peptide induces not only a contracted structure (as reflected by the decrease in mean distance) but also a more compact one. That the narrowing effect on the distribution of peptide **pII** upon phosphorylation is found for both solvents confirms that the associated structural change is intrinsic for the peptide and not solvent-induced.

The combined experimental results obtained from the FRET measurements demonstrate that phosphorylation of **I** leads to a slightly extended donor–acceptor distance, while maintaining the overall flexibility of its random-coiled conformation (similar half-width of the distribution, Figure 2). Phosphorylation converts the serine hydroxyl group in **I** into a sterically more demanding phosphate group, which might intuitively account for the slight elongation in donor–acceptor spacing. In addition, based on well-established secondary-structure preferences,[37] serine is abundant in β-turn segments and facilitates the formation of collapsed structures. Phosphorylated serine bears structurally and sterically a closer resemblance to β-branched amino acids (comparable to valine, isoleucine, and threonine), which are known to have a preference for a β-strand secondary structure, that is, they favor extended conformations.[37,38]

Phosphorylation of peptide **II** results in a more dramatic change in donor–acceptor distance, which signals the formation of a collapsed and more highly structured, rigid phosphorylated peptide. The steric effects or secondary-structure preferences invoked for peptide **I** cannot be held responsible in this case. Instead, we propose that favorable Coulombic and/or hydrogen-bonding interactions between the phosphate group and adjacent amino acid residues impose a structural preference. In particular, our data are consistent with the formation of a salt bridge between the phosphate group with the adjacent arginine and lysine residues, which has been postulated in several accounts.[6,39,40] The planar guanidinium group of arginines is especially predisposed to undergo a double hydrogen-bonding and electrostatic interaction with the doubly negatively charged phosphate group.[2] Note, in this context, arginines are most abundantly found in kinase substrates, where they serve as important recognition sites.[41,42] A salt bridge, like the one tentatively proposed in Scheme 1, would effectively reduce the donor–acceptor distance by favoring a small loop and "pulling" the acceptor closer to the donor. In addition, it accounts for the concomitant structural rigidification.

In order to corroborate the formation of a salt bridge in **pII** experimentally, we performed control experiments at high salt concentrations, conditions under which ion pairing with dissolved ions should compete and thereby weaken a salt bridge. In fact, while the relative steady-state fluorescence intensity of the phosphorylated peptide is nearly 40% higher in water than that of its unphosphorylated counterpart (Figure 1, Table 3), it was found to be practically the same (within 5%) in the presence of 0.3 M sodium phosphate (pH 7.8), or 1 M or 2 M sodium chloride (pH 6.8). This result implies that the postulated salt bridge and associated contracted structure are not favorable at high salt concentrations. However, it must be recalled that added salts have manifold effects on peptide dynamics (increase in solvent viscosity),[23,24] general denaturant effects (cf. Hofmeister series),[43] and potentially on the photophysical parameters (R_0 values),[19] all of which might influence FRET. A detailed study of salt effects on peptide structure and dynamics for a comprehensive series of peptides and salt types is currently in progress.

With respect to potential biological applications of the Trp/Dbo FRET pair, it must be kept in mind that the choice of Trp as an intrinsic amino acid limits the scope of the new method to the investigation of small model peptides. In proteins, including the phosphatases and kinases responsible for dephosphorylation and phosphorylation, the presence of additional Trp residues will interfere in the fluorescence measurement and complicate the quantitative analysis in terms of distances and distance distributions.

Conclusions

The novel Trp/Dbo FRET pair provides structural information on donor–acceptor distances in very short peptides (<20 amino acids) with sub-Å spatial resolution. The corresponding FRET methodology is particularly advantageous for determining distance changes that result from point mutations or small chemical modifications, such as the phosphorylation of serine and threonine residues studied here. Two peptides containing recognition sequences for the protein kinases A and C were investigated by a combination of steady-state and time-resolved FRET. Effective donor–acceptor distances were extracted from the corresponding FRET efficiencies, and distribution functions were derived, which afforded a mean distance and a half-width by assuming a Gaussian function. While phosphorylation of peptide **I** resulted in an slight increase of donor–acceptor separation without a concomitant change in flexibility of the peptide (as judged by the half-width of the distribution), phosphorylation of peptide **II** afforded a contracted and more compact (rigid) structure. The effects of phosphorylation, which could be generalized for both water and propylene glycol as solvent, were attributed to steric effects, variations in secondary-structure preferences, and the formation of salt bridges. Related studies employing the Trp/Dbo FRET pair should offer more detailed microscopic insights into the manifold conformational changes that accompany the methylation or phos-

phorylation of peptides, or their response to external variations like salt effects, pH changes, and temperature. In this context, it should be noted that the collision-induced fluorescence quenching of Dbo by Trp in the same peptides (which requires excitation of Dbo in the near UV) provides complementary information on the dynamics of peptides, namely on their kinetics of end-to-end collision.[22–24]

Experimental Section

Materials: Fmoc-protected Dbo,[22] which is commercially available as Puretime-325 dye (Assaymetrics, Cardiff, UK), was introduced into the particular peptide sequence by solid-phase synthesis (Biosyntan, Berlin, Germany); the purity of the peptides was better than 95%. Nanopure water was used as solvent.

Fluorescence spectroscopy: All measurements were performed at ambient temperature (25 °C). The fluorescence lifetimes of the phosphorylated and unphosphorylated peptides were measured in H_2O and propylene glycol under air by time-correlated single-photon counting (FLS920, Edinburgh Instruments Ltd., Livingston, UK) by using a PicoQuant pulsed LED (PLS-280, $\lambda_{ex} = 280$ nm, $\lambda_{obs} =$ 350 nm, fwhm $\approx$ 450 ps) for excitation. The use of buffer (pH 7.0) instead of H_2O had no significant effect on the fluorescence spectra or lifetimes and was therefore not pursued. The fluorescence decays were fitted according to a biexponential decay model by employing instrument-specific software and reconvoluted with the instrument response function ("lamp profile", obtained with a diffuser). Corrected steady-state emission spectra and intensities ($\lambda_{ex} = 280$ nm) were recorded with a Cary Eclipse (Varian) spectrofluorometer. The optical density of the peptides at the excitation wavelength was adjusted to about 0.10 for the steady-state and to about 0.3 for the time-resolved fluorescence measurements by using a Cary 4000 spectrophotometer (Varian). Optically matched (± 5%) solutions containing a reference peptide with known quantum yield were employed to measure the steady-state FRET efficiencies and calculate the relative fluorescence quantum yields.

Acknowledgements

This work was performed within the graduate program "Nanomolecular Science". The authors would like to thank Dr. Fang Huang, University of Cambridge, for helpful discussions.

Keywords: FRET · kinases · peptides · phosphorylation · time-resolved spectroscopy

[1] T. Hunter, *Cell* **2000**, *100*, 113–127.
[2] L. N. Johnson, D. Barford, *Annu. Rev. Biophys. Biomol. Struct.* **1993**, *22*, 199–232.
[3] P. Cohen, *Eur. J. Biochem.* **2001**, *268*, 5001–5010.
[4] P. E. Wright, H. J. Dyson, *J. Mol. Biol.* **1999**, *293*, 321–331.
[5] L. N. Johnson, R. J. Lewis, *Chem. Rev.* **2001**, *101*, 2209–2242.
[6] C. M. Stultz, A. D. Levin, E. R. Edelman, *J. Biol. Chem.* **2002**, *277*, 47653–47661.
[7] S. W. Vetter, E. Leclerc, *Eur. J. Biochem.* **2001**, *268*, 4292–4299.
[8] W.-J. Dong, J. Xing, J. M. Robinson, H. C. Cheung, *J. Mol. Biol.* **2001**, *314*, 51–61.
[9] H. Watrob, W. Liu, Y. Chen, S. G. Bartlett, L. Jen-Jacobson, M. D. Barkley, *Biochemistry* **2001**, *40*, 683–692.
[10] A. Neininger, H. Thielemann, M. Gaestel, *EMBO J.* **2001**, *2*, 703–708.
[11] M. A. Trakselis, S. C. Alley, E. Abel-Santos, S. J. Benkovic, *Proc. Natl. Acad. Sci. USA* **2001**, *98*, 8368–8375.
[12] P. J. Roach, *FASEB J.* **1990**, *4*, 2961–2968.
[13] G. F. Audette, R. Engelmann, W. Hengstenberg, J. Deutscher, K. Hayakawa, J. W. Quail, L. T. J. Delbaere, *J. Mol. Biol.* **2000**, *303*, 545–553.
[14] A. E. Johnson, *Traffic* **2005**, *6*, 1078–1092.
[15] A. Tholey, A. Lindemann, V. Kinzel, J. Reed, *Biophys. J.* **1999**, *76*, 76–87.
[16] S. E. Wong, K. Bernacki, M. Jacobson, *J. Phys. Chem. B* **2005**, *109*, 5249–5258.
[17] T. Y. Shen, C. F. Wong, J. A. McCammon, *J. Am. Chem. Soc.* **2001**, *123*, 9107–9111.
[18] T. Heyduk, *Curr. Opin. Biotechnol.* **2002**, *13*, 292–296.
[19] H. Sahoo, D. Roccatano, M. Zacharias, W. M. Nau, *J. Am. Chem. Soc.* **2006**, *128*, 8118–8119.
[20] R. B. Pearson, B. E. Kemp, *Methods Enzymol.* **1991**, *200*, 62–81.
[21] J. A. Adams, *Chem. Rev.* **2001**, *101*, 2271–2290.
[22] R. R. Hudgins, F. Huang, G. Gramlich, W. M. Nau, *J. Am. Chem. Soc.* **2002**, *124*, 556–564.
[23] F. Huang, W. M. Nau, *Angew. Chem.* **2003**, *115*, 2371–2374; *Angew. Chem. Int. Ed.* **2003**, *42*, 2269–2272.
[24] F. Huang, R. R. Hudgins, W. M. Nau, *J. Am. Chem. Soc.* **2004**, *126*, 16665–16675.
[25] H. Bakirci, A. L. Koner, W. M. Nau, *J. Org. Chem.* **2005**, *70*, 9960–9966.
[26] R. F. Chen, J. R. Knutson, H. Ziffer, D. Porter, *Biochemistry* **1991**, *30*, 5184–5195.
[27] J. R. Lakowicz, *Principles of Fluorescence Spectroscopy*, Kluwer, New York, **1999**.
[28] R. F. Steiner, E. P. Kirby, *J. Phys. Chem.* **1969**, *73*, 4130–4135.
[29] I.-C. Yeh, G. Hummer, *J. Am. Chem. Soc.* **2002**, *124*, 6563–6568.
[30] D. Roccatano, W. M. Nau, M. Zacharias, *J. Phys. Chem. B* **2004**, *108*, 18734–18742.
[31] J. R. Lakowicz, W. Wiczk, I. Gryczynski, M. L. Johnson, *SPIE* **1990**, *1204*, 192–205.
[32] D. Klostermeier, D. P. Millar, *Biopolymers* **2002**, *61*, 159–179.
[33] Fang Huang, University of Cambridge, has pointed out that a more accurate version of Equation (3) should take into account differences in R_0 values for the different Trp lifetime components, which have been related to different rotamers (cf. ref. [26]). Assuming that the differences of the two lifetime components for the reference peptides **ref-I** and **ref-II** (factor of 2–3) affect the fluorescence quantum yields to the same extent, variations in the R_0 values (square-root-of-6 dependence) of 12–20% could result, and the R_0 values determined in Table 2 would lie in between. Such a refined analysis (which cannot be rigorously implemented due to lack of experimental data for the individual R_0 values of the proposed Trp rotamers) could lead to slight (estimated <10%) variations in the recovered absolute distances, but would not affect the relative trends.
[34] Fittings according to the worm-like chain model afforded the same relative trends in terms of variations in distances and chain flexibility (persistence length).
[35] H. Sahoo, W. M. Nau, **2007**, unpublished results.
[36] CD measurements performed for peptides **I**, **pI**, **II**, and **pII** did not provide evidence for a stable secondary structure either (H. Sahoo, W. M. Nau, *Indian J. Radiat. Res.* **2006**, *3*, 104–112).
[37] M. Levitt, *Biochemistry* **1978**, *17*, 4277–4285.
[38] D. Pal, P. Chakrabarti, *Acta Crystallogr. Sect. D Biol. Crystallogr.* **2000**, *56*, 589–594.
[39] K. Lin, V. L. Rath, S. C. Dai, R. J. Fletterick, P. K. Hwang, *Science* **1996**, *273*, 1539–1541.
[40] G. Waksman, D. Kominos, S. C. Robertson, N. Pant, D. Baltimore, R. B. Birge, D. Cowburn, H. Hanafusa, B. J. Mayer, M. Overduin, M. D. Resh, C. B. Rios, L. Silverman, J. Kuriyan, *Nature* **1992**, *358*, 646–653.
[41] J. R. Knowles, *Annu. Rev. Biochem.* **1980**, *49*, 877–919.
[42] J. F. Riordan, K. D. McElvaney, C. L. Borders, *Science* **1977**, *195*, 884–886.
[43] K. D. Collins, M. W. Washabaugh, *Q. Rev. Biophys.* **1985**, *18*, 323–422.

Received: November 1, 2006
Published online on February 14, 2007

